Journal of the Korean Vacuum Society
Vol. 3, No. 2, June 1994, pp. 147-157

〈기술해설〉

Synchrotron Radiation Induced Photochemical Reactions for Semiconductor Processes

Shi-Woo Rhee

Laboratory for Advanced Materials Processing,
Department of Chemical Engineering, Pohang University of
Science and Technology, Pohang 790-784, Korea
(Received April 10, 1994)

Abstract — Valence or core electron excitations induced by Synchrotron radiation (SR) irradiation and ensuing chemical reactions can be applied for semiconductor processes, i,e.,deposition, etching, and modifications of thin film materials. Unique selectivity can be achieved by this photochemical reactions in deposition and etching. Some materials can be evaporated by SR irradiation,which can be utilized for low temperature surface cleaning of thin films. Also SR irradiation significantly lowers the reaction temperature and photon activated surface reactions can be utilized for direct writing or projection lithography of electronic materials. This technique is especially effective in making nanoscale feature size with abrupt and well defined interfaces for next generation electronic devices.

1. Introduction

Synchrotron radiation (SR) gives intense and stable light covering the wide energy range from hard X-ray to infrared as shown in Fig. 1, and is used in many scientific and engineering applications [1-5]. In the fields of semiconductor fabrication, X-ray lithography has been studied for over ten years as an important application of SR.

Storage rings for the purpose of this industrial application have been constructed in recent years [6] and in this case, it is important, from the view point of efficiency to develop new applications in semiconductor processes other than X-ray lithography. In recent years, SR stimulated photochemical reactions for semiconductor processes have drawn much attention, especially for chemical vapor deposition (CVD) [7-9] including epitaxial growth [10, 11], etching [12-15], doping [16], and surface modifications [17, 18].

Surface reaction dynamics induced by core [19] or valence [20, 21] electron excitation is very interesting from the scientific viewpoint, in the study of SR photochemical reactions. in the valence electron excitation, a localized valence hole (one hole) state is generated first and then relaxes to a stable or metastable state to give a reation product. In the core electron excitation, a core hole state is generated first, then a localized valence hole (two or three holes) state is generated through Auger processes, and the valence hole state relaxes to a reaction product.

Chemical reactions induced by electronic excitations have been studied through the use of electron beams or ion beams but excitation energy cannot be monochromatized in this case and sputtering effects often lead to complex reaction mechanisms. The reaction models proposed by Knotek-Feibelman (KF) [19] and Menzel-Gomer-Redhead (MGR) [20, 21] have been known to be useful in explaining stimulated desorption phenomena induced by core and valence electron excitations, respectively. Monochromatized SR beams may by the most excellent excitation source to study these phenomena or to study more complex relaxation processes including chemical reactions between excited atoms and surrounding molecules.

Numerous studies have been reported on photo

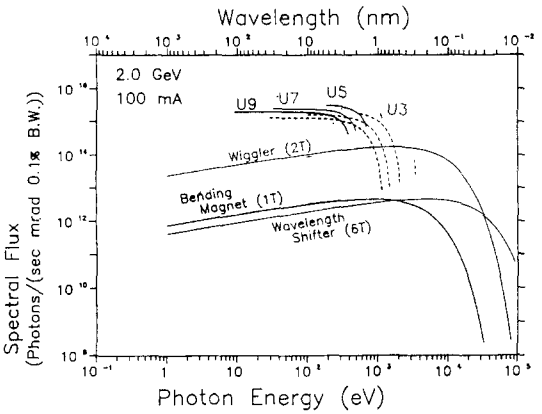

Fig. 1. Intensity distribution of synchrotron radiation from the PAL (Pohang Accelerated Light) storage ring with a bending magnet, a wiggler and an undulator.

excited processes using lasers [22-26] or discharge lamps [27]. Some of theses have been successfully applied for the repair or wiring of semiconductor circuits. However, since many reaction gases used in semiconductor processes have large electronic excitation cross sections in the vacuum ultraviolet (VUV) region with energy higher than about 10 eV, available lasers or discharge lamps cannot excite, or they require high power to excite, these molecules, which inevitably introduces thermal effects. In contrast, SR can excite most of the reaction gases effciently, and can induce almost pure photochemical reactions with negligible thermal effects.

This report reviews recent results of SR CVD, etching, and thin film modifications and characteristics of SR processes are discussed based on these results.

2. Experimental Setup

As an example, Fig. 2 shows a schematic diagram of the beam line and the reaction chamber constructed for the study of photochemical processes [28]. In the VUV range useful for photochemical reaction, we do not have a sufficiently transparent window material. Because of this, the difference in pressure between the reaction chamber using reaction gases and the beam line in the high vacuum is sustained by differential vacuum pumping [28, 29]. Another important parameter of the beam line is horizontal beam divergence of the emitted SR beam. Photon flux is proportional to the usable beam divergence. Differential vacuum pumping usually requires a small diameter beam line duct, which limits the usable beam divergence. Large divergence expands the size of the beam spot at the focusing point due to astigmatism. The size ofthe focusing or reflecting mirror, or the diameter of the beam output port of the SR ring, also limits the usable beam divergence. In this context, an undulator emitting an intense beam with high directivity, is claimed to be ideal in studying photochemical reactions [14, 30].

The reaction chamber attached at the end of the beam line can be equipped with IR, XPS, AES, MS

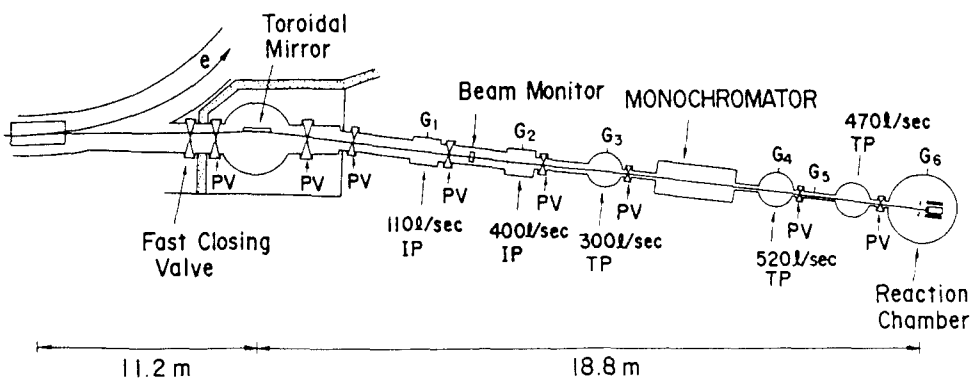

Fig. 2. An example of a beam line and a reaction chamber for the study of photochemical processes [28]. IP, ion pump: TP, turbomolecular pump; PV, pneumatic valve; Gi, cold cathode vacuum gage.

and RHEED for *in-situ* diagnostics and and electron gun for surface cleaning. Base pressure can be as low as 5×10^{-10} Torr. The substrate can be heated from the rear with a thin-film carbon heater or cooled by liquid nitrogen circulation.

3. SR-Excited Chemical Vapor Deposition

3.1. SiN_xH_y Film

Hydrogen-containing silicon nitride film is used as a passivation layer in metal-oxide-semiconductor-field-effect-transistors (MOSFETs). In this application, it has been reported that the hydrogen contained in the film causes degradation of the transistors [31]. Since surface hydrogen is desorbed efficiently by SR excitation, it is expected that the hydrogen content of the CVD film is reduced by SR irradiation.

In the SR CVD on a 100 nm thick SiO_2 film grown on a silicon wafer, deposition occurred preferentially on the irradiated area. SiH_4 (0.02 Torr) and nitrogen (0.1 Torr) concluded that surface excitation is a dominant mechanism. Deposition can also be attributed in part to gas-phase excitation mechanism, since deposition was observed even when the incident beam was parallel to the substrate surface, although the rate was slower than perpendicular arrangement. The hydrogen content of the deposited film was determined from the infrared absorption spectrum. Fig. 3 shows the dependence of hydrogen content on the composition of the film (N/Si) [8]. The reported values of the hydrogen content in a mercury lamp excited CVD film and in a plasma CVD film [32] are given in the same figure. Silicon nitride films with relatively low hydrogen content can be obtained with SR CVD.

It is interesting to compare nitrogen (N_2) and ammonia (NH_3) as a nitrogen source, since NH is an extremely adsorptive gas. Fig. 4 shows the dependence of the film composition (N/Si) on the reaction gas composition (NH_3/SiH_4 or N_2/SiH_4) [33].

With (SiH_4+NH_3) system,(N/Si) of the film suddenly increases at around $NH_3/SiH_4=1$ and saturates sightly above the stoichiometric value. On the other hand, with(SiH_4+N_2) system, the efficiency of nitrogen incorporation is low and (N/Si) increases

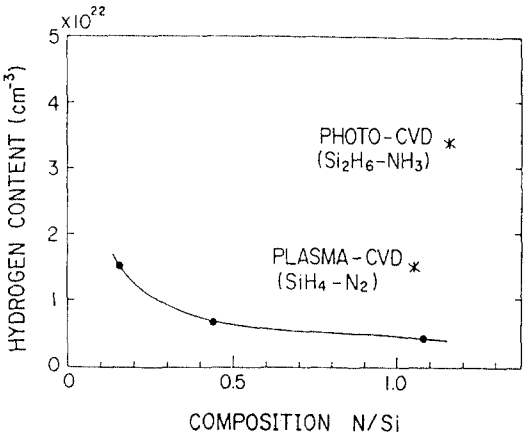

Fig. 3. Dependence of hydrogen content on the N/Si ratio of $Si_xN_yH_z$ film deposited at 190℃ [8].

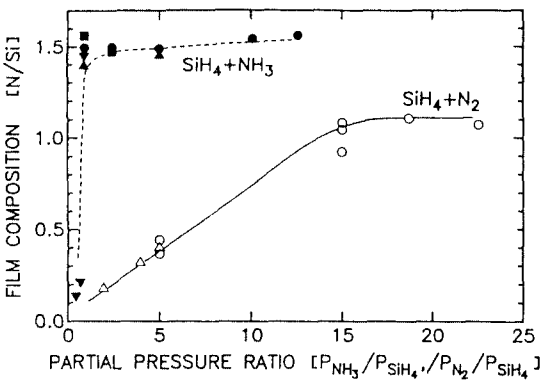

Fig. 4. Effect of the gas phase reactant composition on the composition of the film deposited at 200 ℃. Silane partial pressure was 2×10^{-2} (○, ●), 3×10 A^{-2} (△, ▲), 5×10^{-2} (■) and 0.1 Torr (▼) [33].

in proportion to N_2/SiH_4. Saturation at aroud N/Si= 1 is because of the attenuation of the incident beam intensity due to the absorption by the reaction gas.

Fig. 5 [33] shows the effect of substrate materials and the reactant gas composition on the film composition. The rapid increase in (N/Si) occors at higher value of NH_3/SiH_4 on crystalline silicon substrates than on Si_3N_4. On SiO_2 substrates, a curve similar to Si_3N_4 was obtained. This nonlinear behavior of the composition and its dependence on the substrate material can be qualitatively explained by considering that the efficiency of nitrogen incorpo-

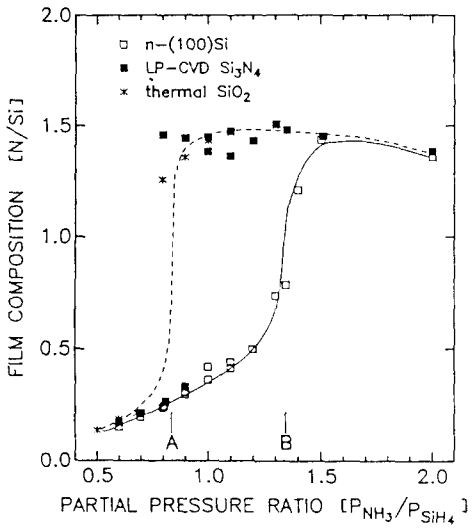

Fig. 5. Effect of gas phase reactant composition and substrate material on the composition of $Si_xN_yH_z$ film deposited at 200℃. Si_2H_6 partial pressure was 1.2×10^{-4} Torr [33].

ration is higher in insulating materials than in semiconducting materials. It must be noted that the substrate material changes during the deposition, since deposition itself changes the substrate surface. It is reported that SiN_x : H film changes from a semiconductor to an insulator at aroud $x=0.3$ [34]. The deposited film is a semiconductor with low NH/SiH values, but changes to an insulator at aroud $NH_3/SiH_4=0.8$, accompanied by an increase in the efficiency of nitrogen incorporation. With *c*-Si substrates, nitrogen incorporation efficiency is low at the initial stage of the deposition and the deposited film changes from a semiconductor to an insulator at a relatively larger value of NH_3/SiH_4. Electronic excitation of the substrate surface is believed to induce the chemical reaction in the (SiH_4+NH_3) system and similar material selectivity is observed in the etching with SF_6.

3.2. Epitaxial Silicon

Temperature lowering in semiconductor processes is now considered to be indispensable in the fabrication of future devices, such as quantum effect devices. For example, it has been pointed out that epitaxial growth at temperatures lower than 300℃ is required to keep the abruptness of silicon/germanium heterojunctions [35]. This is not an easy problem, considering that epitaxial growth of silicon by CVD is conventionally achieved at substrate temperatures higher than 700℃. It has been pointed out that the temperature of CVD silicon epitaxy is limited by the stability of silicon oxide formed by reaction with residual O_2 or H_2O, and that a fairly low temperature (500~700℃) epitaxial growth is achieved by thermal UHV-CVD [36]. But this method has not reached a point to satisfy the above condition. The SR-excited process is a promising technique in this direction because it is a low temperature, low damage and low contamination process.

The observed dependence of epitaxial growth rate on temperature is shown in Fig. 6 [10]. 100% Si_2H_6 (pressure at 1.5×10^{-4} Torr) was fed into the reaction chamber and the Si(100) substrates were used. Surface cleaning was achieved by the conventional thermal desorption method and native oxide was prepared by the wet method [37]. Temperature dependence can be separated into two regions at about 600℃, which was also observed in UHV-CVD using SiH_4 [38, 39]. In the high temperature region, the thermal reaction constant becomes large and chemisorption is the rate-limiting process and the effect of SR irradiation on growth rate is not appreciable. However, at temperatures lower than 600℃, growth rate enhancement due to SR irradiation increases with decreasing temperature. The temperature dependence of epitaxial growth of silicon shows that the reaction is the sum of the photo-assisted process and the thermal process.

In the low temperature region, activation energies are determined to be 31 kcal/mol with SR irradiation and 54 kcal/mol without it, from the data of Fig. 6. without SR irradiation, thermal reaction is rate-limiting and hydrogen desorption such as SiH_2 $(s)\rightarrow Si(s)+H_2(g)$ with $E=59$ kcal/mol can be a possible reaction mechanism [40]. Photo-assisted hydrogen desorption such as

$$SiH_7 \rightarrow *SiH+(n-1)H$$
$$*SiH+SiH \rightarrow H_2(g)+2Si$$

can be considered to be a mechanism operative un-

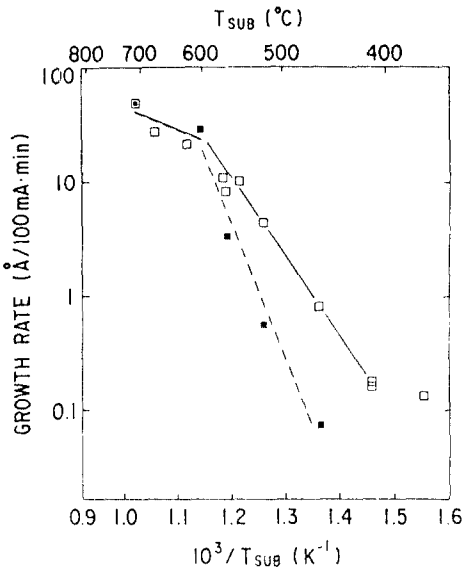

Fig. 6. Epitaxial growth rate of silicon *vs.* the substrate temperature for both thermal (■) and SR irradiation (□) processes [10].

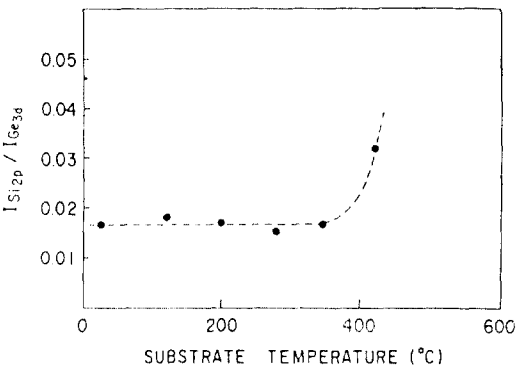

Fig. 7. XPS intensity ratio between Si_{2p} and Ge_{3d} *vs.* Ge(100) substrate temperature. exposure to SiH_2Cl_2 gas is 0.09 Torr×120 s (1.1×10^7 *l*) [45].

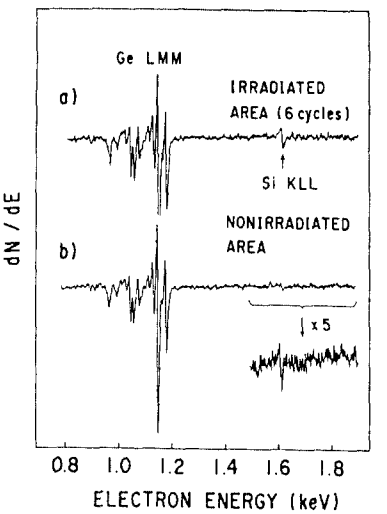

Fig. 8. AE spectra for a) SR irradiated and b) unirradiated area on Ge(100) surface after six cycles of layer-by layer process [45].

der SR irradiation. Good crystal quality was confirmed in all samples by the 2×1 RHEED pattern measured just after the growth.

3.3. Surface Activated Process and Projection Lithography

Some CVD precursors can be molecularly adsorbed at the surface and exhibit a substantial activation barrier to dissociation. Thermal dissociation and desorption of byproducts is the conventional method for deposition but temperatures higher than 500℃ are usually required in this case. This often destroys the structure of the atomic layer itself and makes it difficult to maintain an abrupt interface, Selective area low temperature deposition can be achieved by using incident radiation such as photons, electrons or ions to overcome the activation barrier to dissociation [41]. As a low temperature process, photo stimulated dissociation and desorption is considered to be the most promising technique and the photons in SR have more than enough energy to initiate decomposition of CVD precursor molecules at solid surfaces.

Low temperature surface activated process is expected to be an important technique in such applications as the fabrication of superlattice strucures, direct writing of electronic materials and surface or interface modifications [42-44]. One example is atomic layer epitaxial (ALE) growth of silicon based on this principle. The dependence of the degree of adsorption of SiH_2Cl_2 on the substrate temperature was evaluated on the clean surface of a germanium substrate by using X-ray photoelectronspectroscopy (XPS), as shown in Fig. 7 [45]. It was found that the stable adsorption without deposition is mai-

ntained at temperatures lower than about 400℃ and the reaction in the adsorption is considered to be expressed by

$$SiCl_2H_2(g) \rightarrow SiCl_2(s) + H_2(g)$$

where (g) and (s) represent the gas phase and adsorption state, respectively. Since it is known that atom mixing at the silicon and germanium layer interface starts to occur at about 300℃ [35], the photo-stimulated dissociation and deposition below this temperature is considered to be the best for abrupt silicon/germanium interface formation.

Fig. 8 shows Auger electron (AE) spectra of the surface of a germanium substrate after six cycles of the layer-by-layer process at 300℃ using SR irradiation [45]. Each cycle consists of three procedures: (1) $SiCl_2H_2$ gas exposure of 1.1×10^7 l, 6×10^{-2} Torr, 180s) without SR irradiation; (2) 1 min evacuation pumping to less than 10^{-7} Torr; and (3) 10 min SR irradiation. Spectra (a) and (b) correspond to irradiated and unirradiated areas, respectively. Four to five times as many Si atoms are deposited on the irradiated area as on the unirradiated area. It has been determined that the signal intensity of the silicon KLL transition in the spectrum (a) corresponds to three to five atomic layers. The RHEED pattern for the irradiated area after deposition was the same as the 2×1 reconstruction pattern observed just after the precleaning of germanium substrate. The results indicate that SR irradiation dissociates adsorbed $SiCl_2$ at a sufficiently low temperature to give atomic layer growth of epitaxial silicon.

Single precursors can be used for the deposition of compound films and also in this case, selective area deposition and direct writing, using synchrotron radiation induced surface decomposition, is possible with an appropriate precursor. The possibility of patterned deposition (projection lithography) using SR irradiation of the surface through patterned masks was reported for the direct writing of metal layers, boron and boron carbide films [9, 16, 46]. When the Si(111) surface at room temperature was exposed to both the diethylcarborane and synchrotron white light, the dissociative adsorption and growth of the boron rich boron-carbon film was observed as shown in Fig. 9 [47]. It was pointed out that the boron to carbon ratio of the film was not determined by the composition of the source molecule but the details of the surface dissociation process had a profound influence. The film growth mechanism on the surface was suggested as

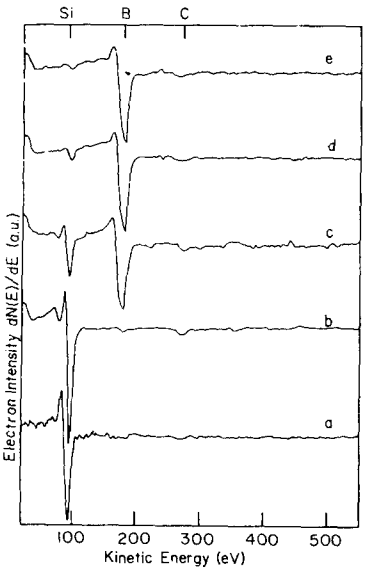

Fig. 9. Synchrotron radiation white light Auger electron spectra of boron-carbon thin films grown on Si(111) at room temperature. a) clean Si (111), b) 225 langmuirs of diethylcarborane without incident X-rays from SR. Substantial film growth is obtained with SR irradiation for c) 100, d) 200 and e) 300 langmuirs [47].

$$(C_2H_2)\ C_2B_4H_6(g) \rightarrow (C_2H_5)_2C_2B_4H_6(s)$$

$$(C_2H_5)_2C_2B_4H_6(s) \rightarrow C_2B_4H_x(s) + 2(C_2H_4)(g)$$

$$C_2B_4H_x(s) \rightarrow 2C(s) + 4B(s)$$

Fig. 10 shows the SEM micrographs of boron rich boron carbide films deposited on Si(111) at room temperature [47]. The patterns are formed by SR enhanced deposition through X-ray lithographic mask and copper wire grid [47]. Potential application of SR to area selective monolayer processes was also demonstratd for boron doping [16].

4. Etching

It was found that silicon and SiO_2 are etched by

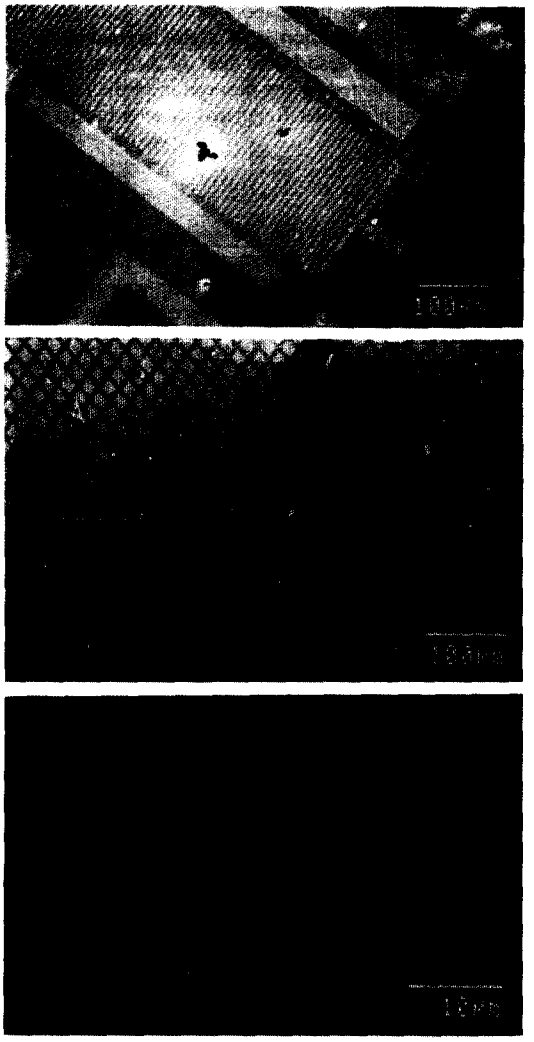

Fig. 10. SEM micrographs of boron rich boron carbide films deposited on Si(111) at room temperature. The patterns are formed by SR enhanced deposition with incident beam passing through an X-ray mask (at the top), through a copper wire grid (in the middle) and the bottom figure is tem times magnification of the middle picture. The deposited film from diethylcarborane shows up brighter than the Si substrate [47].

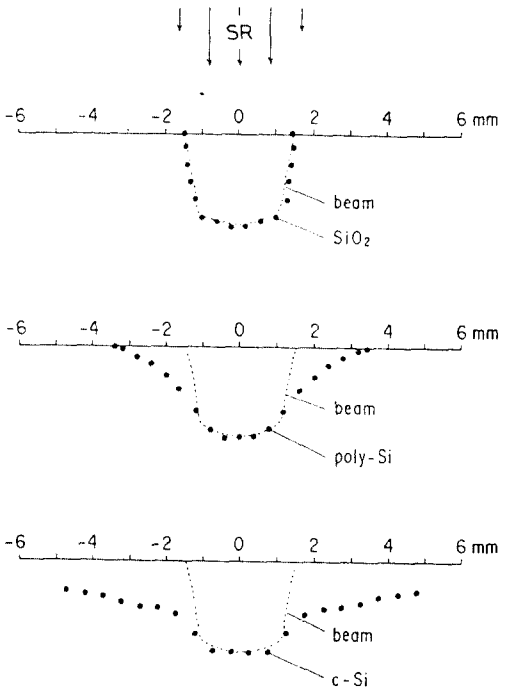

Fig. 11. Observed etch depth profiles of SiO_2, poly-Si and c-Si without oxygen addition, together with SR beem intensity distribution. Pressure of SF_6 was 0.08 Torr and average ring current of the storage ring was 270 mA during the experiment [48].

SR irradiation using SF_6 as a reactant gas [8]. Two kinds of reaction mechanisms are observed, namely surface excitation and gas-phase excitation mechanisms. The gas-phase excitation mechanism is similar to that observed in plasma etching, where etching proceeds by F radicals generated in the gas phase by the plasma reaction. Fig. 11 shows the observed etch profiles for SiO_2, polysilicon and crystalline Si [48]. In case of SiO_2, the etch profile matches with the beam intensity profile, indicating that only the surface excitation mechanism is dominant. Both gas-phase and surface excitation mechanisms contribute to poly-Si etching and for c-Si, gas phase excitation is dominant. The gas-phase excitation has been found to be suppressed by adding a small percentage of oxygen to SF_6 [48]. It was observed that etch rate of c-Si is almost suppressed by the addition of oxygen, while that of SiO_2 is not. This can be utilized to get high selectivity of Si and SiO_2 etching [8, 48].

It has been pointed out that the effect of doping on the etch rate of poly-Si is quite different from plasma etching [49] or laser etching [50]. For both n-and p-types, the SR etch rate decreases with inc-

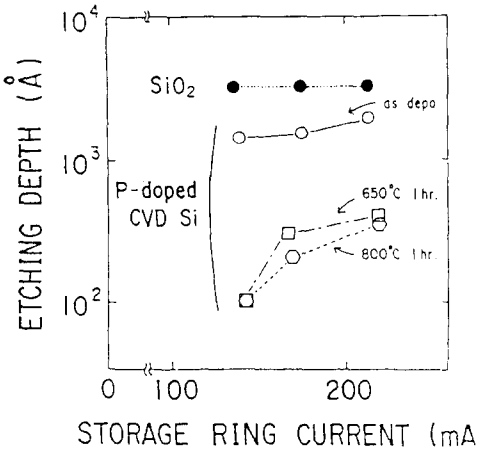

Fig. 12. Etch rate of poly-Si as a function of sheet resistance controlled by P or B doping. SF_6 total pressure is 0.08 Torr, substrate temperature is 300 K and storage ring durrent is 170 mA. Two kinds of beam line optics were used: the system with only one toroidal mirror and the system with one toroidal mirror and a pair of platinum-coated plane mirrors with grazing incidence angle of 5° [51].

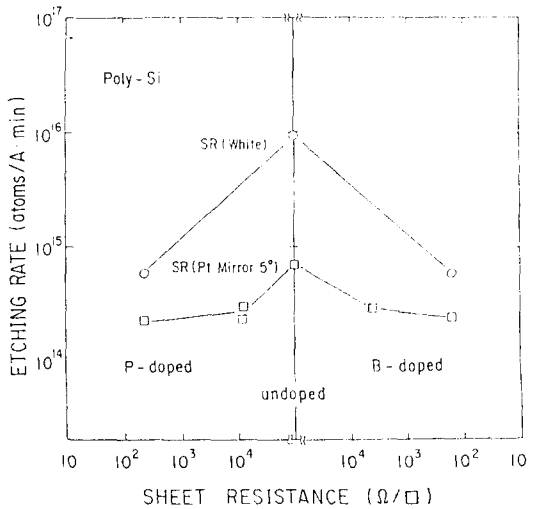

Fig. 13. Etch rate of SiO_2, P-doped poly-Si and amorphous silicon as a function of storage fing current for a constant dose, 2.2×10^4 mA min (ring current x etch time). P-doped CVD silicon was amorphous as deposited, and polycrystalline after annealing at 650℃ or 800℃ [52].

reasing dopant doncentrations, as shown in Fig. 12 [51, 52]. For plasma etching using XeF_2 gas, the

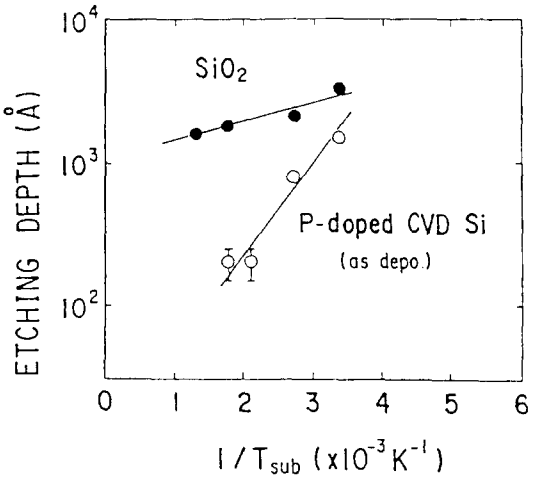

Fig. 14. Etch rate of SiO_2 and poly-Si *vs.* temperature. Dose was 2.2×10^4 mA min and SF_6 pressure was 0.13 Torr.

etch rate of *n*-type silicon is larger than that of undoped of *p*-type silicon, and the rate increases with increasing *n*-type dopant concentrations [49]. The dependence of etch rate on conductivity is not so significant in the excimer laser etching of *c*-Si using NF gas. Another characteristics of SR etching of poly-Si and amorphous silicon is the dependence of etch rate on beam intensity. For SiO_2, the etch rate depends linearly on beam intensity, *i.e.*, the etch rate per unit photon flux is constant. However, for poly-Si or amorphous silicon, it has been found that etch rate per unit photon flux increases with increasing beam intensity, as shown in Fig. 13 [52]. Insulating marterials are etched at a higher rate than semiconducting materials and the etch rate of silicon increases with degradation in crystallinity.

Fig. 14 shows the dependence of etch rate of SiO and poly-Si on temperature. This temperature dependence indicates that the rate of SiO and poly-Si on temperature. This temperature dependence indicates that the rate determining step in the reaction is the direct photo-excitation process. Material selectivity is qualitatively explained by assuming that the reactive center, which is the valence hole state itself or some state generated through the relaxation of the valence hole state, is easitly quenched in *c*-Si or highly condutive poly-Si before the fluorination reaction occurs. On the other hand, in insu-

lating materials or low-conductive poly-Si, the lifetime of such a reactive center is sufficiently long to induce the fluorination reaction and desorption of SiF_n. SR etching using reaction gases such as chlorine [12, 15], oxygen [13] and hydrogen has also been reported. The usefulness of the undulator light was demonstrated in investigating wavelength dependence in etching experiments using SF_6 [14].

5. Evaporation and Surface Modification

It has been found that SiO_2 evaporates at relatively low temperatures on SR irradiation under UHV conditions [53, 54]. The evaporation rate increases gradually with increasing temperature, and the rate of increase becomes much larger above 500℃, as shown in Fig. 15. Evaporation occurs only on irradiated areas and material selectivity can be obtained because neither polycrystalline nor crystalline silicon are evaporated. It is noteworthy that effective activation energy gradually increases with increasing temperature. It is roughly evaluated to be 17.7 kcal/mol and 5.2 kcal/mol above and below 450℃, respectively. Contribution of many kinds of metastable species is a possible explanation for the gradual change of activation energy. For both SiO_2 evaporation and epitaxial growth, further experiments such as observation of desorption species, are necessary to understand the reaction mechanism.

Thermal evaporation of SiO_2 is used as a surface cleaning method for silicon substrates [37]. Therefore, SR evaporation of SiO_2 is expected to be applicable to low temperature surface indicating the cleanliness and good crystal quality. The above experiments indicate that the SR evaporation phenomena can, in principle, be applicable to the surface cleaning of silicon substrates for silicon epitaxial growth, However, it must be noticed that the cleaning time is very long compared with the time estimated from the evaporation rate of bulk SiO as shown in Fig. 15 and the thickness of native oxide, usually less than 20 A. This indicates that either the evaporation rate of a thin SiO_2 film on c-Si is slow compared with that of thick SiO_2, or it slows down near the SiO_2/Si boundary. A similar phenomenon has been observed in the etching with SF_6

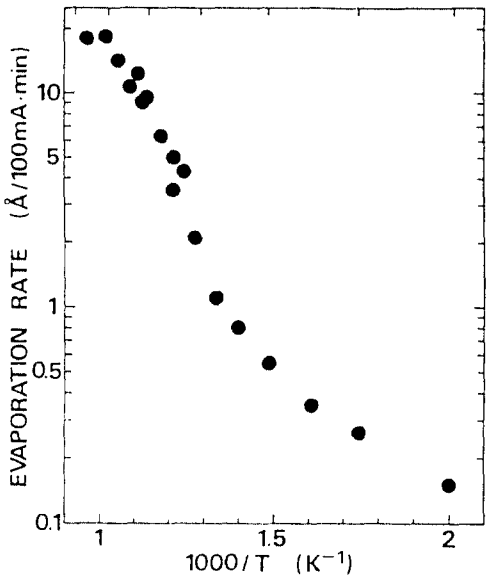

Fig. 15. Dependence of SiO_2 evaporation rate on substrate temperature for a ring current of 100 mA [53].

gas. The etching rate of c-Si is decreased to almost zero by adding oxygen to SF_6 [8, 48]. This effect in the unirradiated area is explained by the formation of a surface oxide layer, which protects the silicon surface from the etching reaction of F radicals generated by gas-phase excitation. The disappearance of etch rate in the irradiated area, however, cannot simply be explined by this mechanism, since it is known that bulk SiO_2 is easily etched by the surface excitation mechanism. This contradiction is also explained, if the etch rate of thin SiO_2 film on c-Si is assumed to be much slower than that on bulk SiO_2. This also applies to SF_6 etching. As for the selectivity where the etch rate of Si decreases with either inceasing conductivity or crystallinity, one possible explanation for these boundary effects is that the lifetime of reactive centers generated close to the substrate surfaces by SR irradiation is shortened due to the influence of c-Si substrate.

The silicon surface was found to be nitrided by SR irradiation under ammonia (NH_3) gas at low temperatures [17, 18], which can be used for the modification of thin film surfaces.

Acknowledgments

The author would like to thank PLS (Pohang Light Source) for the financial support of this research through the user training program.

References

1. C. Kunz, *Synchrotron Radiation-Techniques and Applications*, Ed., Springer-Verlag, 1979.
2. G. Margaritondo, *Introduction to Synchrotron Radiation*, Oxford University Press, 1988.
3. C. R. A. Catlow and G. N. Greaves, *Applications of Synchrotron Radiation*, Eds., Chapman and Hall, 1990.
4. R. Clarke, J. Gland and J. H. Weaver, *Synchrotron Radiation in Materials research*, Proc. of Materials Research Society, Vol. 143, 1989.
5. D. L. Perry, N. D. Shinn, R. L. Stockbauer, K. L. D'Amico and L. J. Terminello, *Applications of Synchrotron Radiation Techniques to Materials Science*, Proc. of Materials Research Society, Vol. 307, 1993.
6. T. Hosokawa, T. Kitayama, T. Hayasaka, S. Ido, Y. Uno, A. Shibayama, J. Nakata, K. Nishimura and M. Nakajima, *Rev. Sci. Instrum.* **60**, 1783 (1989).
7. H. Kyuragi and T. Urisu, *J. Appl. Phys.* **61**, 2035 (1987).
8. T. Urisu and H. Kyuragi, *J. Vac. Sci. Technol.* **B5**, 1436 (1987).
9. D. C. Mancini, S. Varma, J. K. Simons, R. A. Rosenberg and P. A. Kowben, *J. Vac. Sci. Technol.* **B8**, 1804 (1990).
10. J. Takahashi, Y. Utsumi, H. Akazawa, I. Kawasima and T. Urisu, *Appl. Phys. Lett.* **58**, 2776 (1991).
11. H. Hochst and M. A. Engelhardt, *J. Vac. Sci. Technol.* **B8**, 686 (1990).
12. N. Hayasaka, A. Hiraya and K. Shobatake, *Jpn. J. Appl. Phys.* **26**, L1110 (1987).
13. H. Kyuragi and T. Urisu, *Appl. Phys. Lett.* **50**, 1254 (1987).
14. K. Shobatake, H. Ohashi, K. Fukui, A. Hiraya, N. Hayasaka, H. Okano, A. Yoshida and H. Kume, *Appl. Phys. Lett.* **56**, 2189 (1990).
15. S. Terakado, J. Nishino, M. Morigami, M. Harada, S. Suzuki, K. Tanaka and J. Chikawa, *Jpn. J. Appl. Phys.* **29**, L709 (1990).
16. R. A. Rosenberg, F. K. Perkins, D. C. Mancini, G. R. Harp, B. P. Tonner, S. Lee and P. A. Dowben, *Appl. Phys. Lett.* **58**, 607 (1991).
17. F. Cerrina, B. Lai, G. M. Wells, J. R. Wiley, D. G. Kilday and G. Margaritondo, *Appl. Phys. Lett.* **50**, 533 (1987).
18. B. Lai, R. Nachman, A. K. Ray-Chaudhuri and F. Cerrina, *Solid tate Commun.* **71**, 721 (1989).
19. M. L. Knotek and P. J. Feibelman, *Phys. Rev. Lett.* **40**, 964 (1978).
20. D. Menzel and R. Gomer, *J. Chem. Phys.* **41**, 3311 (1964).
21. P. A. Redhead, *Can. J. Phys.* **42**, 886 (1964).
22. D. J. Ehrlich, R. M. Osgood, Jr and T. F. Deutsch, *IEEE J. Quantum. Electron.* **QE16**, 1233 (1980).
23. T. J. Chuang, *J. Vac. Sci. Technol.* **18**, 638 (1981).
24. M. Hanabusa, *Mat. Sci. Rep.* **2**, 51 (1987).
25. V. M. Konnelly and J. A. McCaulley, *Appl. Pyhys. Lett.* **54**, 2456 (1989).
26. S. Yokoyama, Y. Yamakage and M. Hirose, *Appl. Phys. Lett.* **47**, 389 (1985).
27. A. Yamada, A. Satoh, K. Konagai and K. Takahashi, *J. Appl. Phys.* **65**, 4268 (1989).
28. T. Urisu, H. Kyuragi, Y. Utsumi, J. Takahashi and M. Kitamura, *Rev. Sci. Instrum.* **60**, 2157 (1989).
29. J. Janes and N. Lutz, *Appl. Optics* **28**, 3327 (1989).
30. J. M. Ortega, M. Billardon, G. Jezequel, P. Thiry and Y. Petroff, *J. Phys.* **45**, 1883 (1984).
31. R. B. Fair, and R. C. Sun, *IEEE Trans. Electron Devices* **28**, 83 (1981).
32. T. H. Wood, J. C. White and B. A. Thacker, *Appl. Phys. Lett.* **42**, 408 (1983).
33. H. Kyuragi and T. Urisu, *J. Electrochem. Soc.* **138**, 3412 (1991).
34. H. Kurata, M. Hirose and Y. Osaka, *Jpn. J. Appl. Phys.* **20**, L811 (1981).
35. S. S. Iyer, P. R. Pukite, J. C. Tsang and M. W. Copel, *J. Crystal Growth* **95**, 439 (1989).
36. B. S. Meyerson, E. Ganin, D. A. Smith and T. N. Nguyen, *J. Electrochem. Soc.* **133**, 1232 (1986).
37. A. Ishizaka and Y. Shiraki, *J. Electrochem. Soc.* **133**, 667 (1986).
38. M. Liehr, C. M. Greenlief, S. R. Kasi and M. Offenberg, *Appl. Phys. Lett.* **56**, 629 (1990).
39. F. Hirose, M. Suemitsu and N. Miyamoto, *Ipn. J. Appl. Phys.* **29**, L83 (1990).
40. R. J. Buss, P. Ho, W. G. Breiland and M. E. Coltrin, *J. Appl. Phys.* **63**, 2808 (1988).
41. P. A. Dowben, J. T. Spencer and G. T. Stauf, *Mater. Sci. Engin.* **B2**, 297 (1989).

42. J. Nishizawa, H. Abe and T. Kurabayashi, *J. Electrochem. Soc.* **132**, 1197 (1985).
43. Y. Takahashi, H. Ishii and K. Fujinga, *J. Electrochem. Soc.* **136**, 1826 (1989).
44. Y. Takahashi, Y. Sese and T. Urisu, *Jpn. J. Appl. Phys.* **28**, 2387 (1989).
45. Y. Takahashi and T. Urisu, *Jpn. J. Appl. Phys.* **30**, L209 (1991).
46. F. K. Perkins, R. A. Rosenberg, S. Lee and P. A. Dowben, *J. Appl. Phys.* **69**(7), 4103 (1991).
47. F. K. Perkins, M. Onellion, S. Lee, Kongqi Li, J. Mazurowski and P. A. Dowben, *Appl. Phys.* **A54**, 442 (1992).
48. Y. Utsumi, J. Takahashi and T. Urisu, *J. Vac. Sci. Technol.* **B9**, 2507 (1991).
49. F. A. Houle, *J. Chem. Phys.* **79**, 4237 (1983).
50. Y. Horiike, N. Hayasaka, M. Sekine, T. Arikado, M. Nakase and H. Okano, *Appl. Phys.* **A44**, 313 (1987).
51. J. Takahashi, Y. Utsumi and T. Urisu, *Mat. Res. Soc. Symp. Proc.* **158**, 53 (1990).
52. J. Takahashi, Y. Utsumi and T. Urisu, *J. Appl. Phys.* **70**, 2958 (1991).
53. H. Akazawa, Y. Utsumi, J. Takahashi and T. Urisu, *Appl. Phys. Lett.* **57**, 2302 (1990).
54. M. Niwano, H. Katakura, H. Takakuwa and N. Miyamoto, *Appl. Phys, Lett.* **56**, 1125 (1990).